

Binding of Reactive Brilliant Red to Human Serum Albumin: Insights into the Molecular Toxicity of Sulfonic Azo Dyes

Wei-Ying Li¹, Fang-Fang Chen¹ and Shi-Long Wang^{2,*}

¹State Key Laboratory of Pollution Control and Resource Reuse, Tongji University, Shanghai, 200092, China; ²School of Life Sciences and Technology, Tongji University, Shanghai, 200092, China

Abstract: The non-covalent interaction of reactive brilliant red (RBR) as a representative of sulfonic azo compounds with human serum albumin (HSA) was investigated by a combination of UV-VIS spectrometry, fluorophotometry, circular dichroism (CD) and isothermal titration calorimetry (ITC) technique. The thermodynamic characterization of the interaction was performed. The saturation binding numbers of RBR on peptide chains were determined and the effects of electrolytes and temperature were investigated. The ionic interaction induced a combination of multiple non-covalent bonds including hydrogen bonds, hydrophobic interactions and van der Waals force. A three-step binding model of RBR was revealed. The binding of RBR molecules might occur on the external surface of HSA via electric interaction when the mole ratio of RBR to HSA was less than 40 and RBR molecules entered the hydrophobic intracavity of HSA when the ratio was more than 40. Moreover, RBR binding resulted in a conformational change in the structure of HSA or even the precipitation of HSA and inhibited its function accordingly. The possible binding site and the conformational transition of HSA were hypothesized and illustrated. This work provides a new insight into non-covalent interaction between a sulfonic azo compound and protein, which may be further used to investigate the potential toxicity of azo dyes.

Keywords: Non-covalent interaction; reactive brilliant red; human serum albumin.

INTRODUCTION

The interaction of small molecule with biological macromolecule is one of the most extensively studied phenomena in biophysical research. The binding subjects include a vast range of important biochemical phenomena, for example, the reversible binding of oxygen by myoglobins and the non-covalent association of serum albumin with fatty acids and other compounds containing nonpolar groups [1-3]. In this respect, many drugs [4], bilirubin [5], fatty acids [6] must be carried to their sites of action to exert their activity and normally this function is performed by blood transport proteins, such as the globular protein human serum albumin (HSA). HSA has been widely used as a model protein for studying the interaction between proteins and different surface substrates [4] because it constitutes approximately half of the total blood protein, acting as a carrier for fatty acids [6] and several amphiphiles from the bloodstream to tissues. HSA is also responsible for 80% of the colloid osmotic pressure of plasma (25-33 mm Hg) [7]. HSA is an asymmetric heart-shaped molecule with sides of 8 nm and a thickness of 3 nm, and it consists of 585 amino acids in a single polypeptide chain of molecular weight 66.5 kDa [6]. The two heart "lobes" contain two HSA binding sites, which consist almost exclusively of hydrophobic side chains, while the outside of the molecule contains most of the polar groups. The globular structure of HSA is composed of three main domains that are loosely joined together through physical forces and six sub-domains that are wrapped by disulfide bonds. HSA contains

17 disulfide bridges and one free -SH group. Thus, it is expected that upon adsorption some possible structural deformation may occur as a result of either the interaction between the protein molecule and the substrate, steric or electrostatic effects within the adsorbed layer, or a combination of both processes [4, 8]. Recently, studies have been conducted on the binding of organic contaminants or toxins to HSA e.g. dye [9], methyl parathion [10] and arsenic [11]. The binding interaction induced by these compounds can deform the structure of HSA, leading to a decreasing transport rates or decreasing ability to pass through biological barriers.

One representative of aromatic azo compounds, reactive brilliant red (RBR) is extensively used as the textile dye for cloth coloring. Due to its bright red colour, and fast fixation, sometimes it is even added illegally into food and skin cosmetics. Thus, it may enter human bodies by food intake and skin absorption. Azo compounds with an aromatic ring linked by an azo bond to a second naphthalene or benzene ring can be reduced by azo reductases produced by intestinal bacteria and, to a lesser extent, by enzymes of the cytosolic and microsomal fractions of the liver to produce aromatic amines, some of which are known carcinogens [12]. Although such azo compounds may not be directly carcinogenic, they may bind and aggregate directly with proteins, such as enzymes by molecular interactions [9, 13], altering protein function or enzyme activity and thus causing toxicity. RBR is potentially toxic to human if it exists in food and skin cosmetics. In the present work, we undertook an attempt to clarify the general principles involved in the effect of non-specific binding of a sulfonic aromatic compound RBR on HSA by using UV-VIS spectrometry, fluorophotometry, circular dichroism (CD) and isothermal titration calorimetry

*Address correspondence to this author at the Siping Road 1239, Shanghai, 200092, China; Tel: 86-21-65982595; Fax: 86-21-65982595; E-mail: wsl@tongji.edu.cn

(ITC) technique. UV-VIS and CD were used to characterize the binding of RBR to HSA at pH 2.19, 2.86 and 3.39, and the spectral correction technique [14] was used to elucidate the mechanism of interaction.

MATERIALS AND METHODS

Instruments and Materials

The absorption spectra of RBR and its protein solutions were recorded with a Model Lambda-25 spectrometer (Perkin-Elmer Corp., Shelton, USA). The spectrometer was computer controlled using UV WinLab software (Version 2.85.04). A Model F-4500 fluorospectrophotometer (Hitachi High-Technology Corp., Tokyo, Japan) was used to measure the fluorescence of protein solutions in the presence of RBR. The isothermal titration calorimeters (ITC) experiments were carried out on a Model VP-ITC system (MicroCal Inc., USA) with VP-Viewer 2000 (Version 1.04.0018) and Origin software (version 7.0). A Model J-715 CD spectropolarimeter (JASCO Corp., Tokyo, Japan) was used to measure the secondary conformation of proteins. 0.100 g of HSA (A-1653, purity 96-99%, Sigma Reagents Co.) was dissolved in 500 ml of deionized water to get 0.200 mg/ml and stored at 2-8 °C. RBR raw material (approximately 70% of content, Shanghai Dyestuff Factory, China) was re-crystallized for three times in ethanol to yield pure RBR crystals (over 98% of content), which was examined with HPLC. A standard RBR solution (0.350 mmol/l) was prepared in deionized water with these RBR crystals. These solutions were stored in the refrigerator freezer at less than 4 °C. A series of Britton-Robinson (B-R) buffers, pH 1.96, 2.19, 2.51, 2.86, 3.06, 3.39, 3.90 and 4.14 were prepared to adjust the acidities of solutions.

Photometric Characterization of the RBR-HSA Interaction

All studies were carried out in a 10.0 ml calibrated flask containing a known volume of 0.2 mg/ml HSA solution, 1.0 ml of B-R buffer (pH 2.19, 2.86 or 3.39) and a known volume of 0.350 mmol/l RBR. The solution was diluted to 10.0 ml with deionized water and mixed thoroughly. After reacting for 5 min, the absorbances A_{λ_2} and A_{λ_1} of the HSA-RBR solutions and $A_{\lambda_2}^0$ and $A_{\lambda_1}^0$ of the reagent blank (without HSA) were measured at 577 nm (λ_2) and 542 nm (λ_1) against water using UV-VIS. The parameters of the spectral correction technique [14], A_c , η and γ of each solution were calculated.

CD Measurement of HSA Conformation in Presence of RBR

B-R buffer (1 ml, pH 2.19, 2.86 or 3.39) was mixed with 0.7 ml of HSA solution (0.20 mg/ml) in four flasks, then a series of RBR, 0.000, 0.007, 0.014 and 0.018 mmol/l, were added into the former four flasks, respectively. The solutions were diluted to 10.0 ml with deionized water. Each sample was allowed to equilibrate for 5 min before measurement. CD spectra were taken on a spectropolarimeter with a cell (1 cm in length) at 25 °C and data collected at a scan rate of 100 nm/min. Three scanning spectra were averaged and data were linearly smoothed by the addition of 5 adjacent points. The mean residue ellipticity (θ) of HSA was measured be-

tween 190 and 250 nm. From the variation of θ , the relative contents of secondary structure forms of HSA, such as α -helix, β -sheet, β -turn and random coil, were estimated.

Fluorescence Measurement of the RBR-HSA Interaction

B-R buffer (1.0 ml, pH 2.19, 2.86 or 3.39) and 5 ml of 0.2 mg/ml HSA were mixed with 0.00 - 24.5 μ mol/l of RBR. The solutions were diluted to 10 ml with deionized water and their fluorescence intensities measured at the excitation wavelength (280 nm) and the emission wavelengths (300-450 nm). All spectra were recorded in a 1 cm stirred cell with the excitation and the emission slit width set at 10 nm.

ITC Determination of the RBR-HSA Interaction

ITC experiments were carried out as follows. The RBR solutions (2.5 mmol/l at pH 2.19, 2.86 and 3.39, respectively) were injected about 45 times in 6- μ l increments at 190-s intervals into the isothermal cell containing HSA (0.002 mmol/l at pH 2.19, 2.86 and 3.39). The cell temperature was kept at 37 °C. Heats of dilution of RBR, obtained separately by injecting RBR into the buffer, were used to correct the raw data. The corrected heats were divided by the number of moles injected and analyzed using the Origin software (V7.0) supplied by the manufacturer. The titration curve was fitted by a nonlinear least-squares method and N , K , ΔH and ΔS determined.

RESULTS AND DISCUSSION

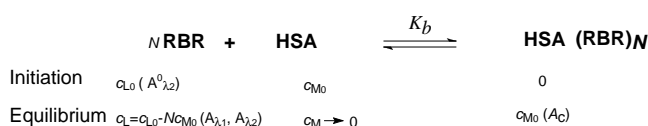
pH Dependence of the RBR-HSA Interaction

RBR is an aromatic azo compound that can form a bright red solution when dissolved in water and it is able to react with HSA to form a violet complex. The absorption spectrum shows an obvious red-shift of RBR spectrum. From the absorption spectra of HSA-RBR solutions (Fig. 1A), the interval between the positive peak and the negative valley increases with increasing acidity of solution. This may be explained reasonably from the occupancy of the acidic amino acid residues (AARs) (Glu and Asp). There are 98 acidic AARs (Glu and Asp) and 99 basic AARs (Lys, His and Arg) in 585 AARs of HSA. The dissociation constants (pK_R) of the side groups (Rs) of these AARs are 10.53 for Lys, 6.00 for His, 12.48 for Arg, 3.65 for Asp and 4.25 for Glu. The distribution of $-R^-$ (negatively charged side groups of Glu and Asp) and $-RH$ groups (side groups of Glu and Asp without charge) is calculated when pH is less than 3.65, e.g. the molar number of $-R_{Glu}^-H$ is more than 4 times that of $-R_{Glu}^-$ and that of $-R_{Asp}^-H$ more than that of $-R_{Asp}^-$. In such an acidic media, almost all of the side groups of the basic AARs are positively charged. It is favorable for RBR anions to bind to HSA. The structural change of RBR (L) from L^{2-} to HL^- and H_2L in an acidic solution is unfavorable for the interaction of RBR with HSA. Thus, there is an optimal pH at which the maximum number of RBR molecules binds to HSA. From curves in Fig. (1A), the strongest binding between RBR and HSA is at pH 2.19. In order to compare the interactions of RBR with HSA in various pH media, three buffer solutions, pH 2.19, 2.86 and 3.39 were used. Both 577 (λ_2) and 542 nm (λ_1) were selected as the measurement wavelengths that most clearly indicated the binding process.

Actually, various tissues of human body have discrepancy in pH e.g. pH 1 - 3 in gastro, pH 3 - 4 in vagina, pH 4 - 5 in duodenum, approximate pH 5 on skin and pH 7.4 in blood. From Fig. (1A), the most sensitive binding of RBR is located in the pH scope of normal gastric juice. Thus, the effect of RBR on the activity of protein or enzyme in gastro tissue should be the most serious when RBR was used as a food additive. However, use of the beauty skin agents especially those containing fruit acid and salicylic acid, favorable for sterilization and inflammation will cause the increase of skin acidity. Besides, it is possible for air pollution such as acidic rains to make skin more acidic. Thus, the pH of skin often approaches 4.0 in many cases and it is just close to the above optimal pH of RBR for binding to peptide chains. RBR could cause more health risk if it was used as the dyeing of clothes or as an additive of a beauty skin agent.

Photometric Characterization of the RBR-HSA Interaction

The interaction of RBR (L) with HSA (M) can be summarized below:



Both c_{L0} and c_{M0} are the initial mole concentration of RBR. The symbol c_L is the equilibrium concentration of RBR, K_b the binding constant in (M^{-1}) and N the saturation binding number of RBR in HSA. Both A_{λ_2} and A_{λ_1} are the absorbances of the HSA-RBR solution, measured at wavelengths λ_2 and λ_1 . The symbol A_{λ_2} is the absorbance of RBR solution at λ_2 and A_c is that of the binding product. The spectral correction technique was applied [14] and the effective fraction (η) of RBR and the molar ratio (γ) of RBR bound to HSA were calculated by the following relations:

$$\eta = \frac{A_c - A_{\lambda_2}}{A_{\lambda_2}^0} + 1 \quad \dots\dots\dots (1)$$

and

$$\gamma = \eta \times \frac{c_{L0}}{c_{M0}} \quad \dots\dots\dots (2)$$

where

$$A_c = \frac{A_{\lambda_2} - \beta A_{\lambda_1}}{1 - \alpha\beta} \quad \dots\dots\dots (3)$$

The symbols α and β are the correction constants. The absorbance ratio (A_{542nm} / A_{577nm}) of the HSA-RBR solutions was measured at 542 and 577 nm, and their values are shown in Fig. (1B). The ratio value decreases with increasing HSA concentration and approaches a constant value of 1.51 when HSA is over 0.75 μM . This indicates that more and more RBR molecules bound to HSA until no excess RBR existed in solution. Thus, this constant minimum could be used as the α value for characterizing the binding product. The β value of RBR corresponds to the A_{577nm} / A_{542nm} ratio in the absence of HSA, which is located at the beginning of curve

B. By measuring a series of RBR solutions containing known concentrations of HSA, A_c , η and γ were calculated according to Eqs. 1 - 3 above. The variation in γ of RBR is shown in Fig. (2); where γ increases with increasing RBR concentrations. Moreover, the value approaches the following maximal constants: approximately 83, 73 and 64 from curves 1 - 3 when c_{L0} is more than 35 mmol/l. These maximum values directly reveal that the binding of RBR with HSA may have reached saturation. These values are further examined and corrected in the following experiments. HSA contains 99 of basic AARs such as Lys, His and Arg and 98 of acidic AARs, such as Glu and Asp [15]. RBR may bind to only one basic AAR due to the steric hindrance if two basic AARs are adjacent to each other, e.g. H9 and R10, and H105 and K106. The N of RBR at pH 2.19 approaches the number of basic AARs, so the ion-pair attraction plays the preliminary position-fixing role [14, 16] in the interaction of RBR with HSA. The dissociation constants (pK_R) of their side chain groups (Rs) are 10.53 for Lys, 6.00 for His, 12.48 for Arg, 3.65 for Asp and 4.25 for Glu. Almost all Rs of basic AARs are with the positive charges, e.g. $-NH_3^+$, $=NH_2^+$ and $>NH_2^+$ when pH is less than 6.00. Thus, it is favorable for electric binding of RBR anions. However, the Rs of Asp residue exists in $-CH_2COOH$ form only when pH is much less than 3.65. Otherwise, the $-CH_2COO^-$ anions occupy a high fraction in HSA and they will repulse the binding of RBR anions. Thus, N value decreases with the increase of pH. In addition, HSA precipitation was observed when the ratio of c_{L0} / c_{M0} was more than 100 and the precipitation was disappeared if re-mixed thoroughly. The possible reason is that the excess RBR bridged between HSA via electric interaction to form a supramolecular aggregate. Therefore, the ratio of c_{L0} / c_{M0} was maintained in less than 100.

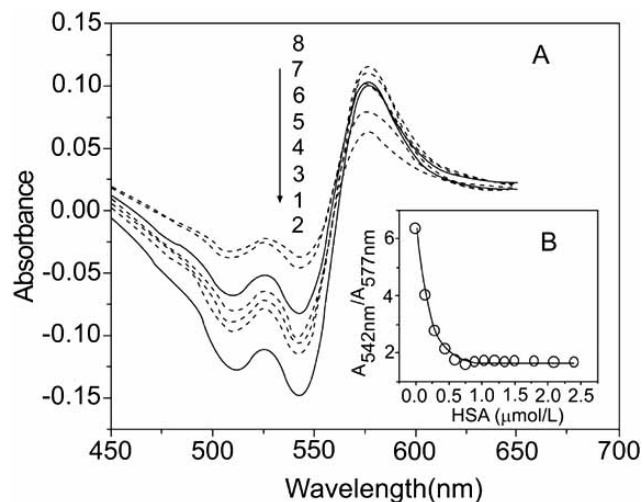


Figure 1. (A) Absorption spectra of the HSA-RBR solutions containing 0.035 mmol/l RBR and 0.02 mg/ml HSA at a series of pH, 1.96, 2.19, 2.51, 2.86, 3.06, 3.39, 3.90 and 4.14, all measured against the reagent blank without HSA; (B) variation of the absorbance ratio (A_{542nm} / A_{577nm}) of the HSA-RBR solutions at pH 2.19, where RBR was 0.035 mmol/l.

Effects of Electrolyte and Temperature

The stability of non-covalent interaction is always affected by various physicochemical conditions such as pH, ionic strength and temperature [17]. The effect of electro-

lytes on γ is shown in Fig. (3A). With increasing electrolyte, γ decreases in three pH media. Its value in 1.0 mol/l electrolyte is less than 30% of that in the absence of electrolyte at pH 2.19, 2.86 and pH 3.39. This is due to the Debye-Huckel screening, where the Debye length is inversely proportional to the square root of the ionic strength of solution [18]. From curves 1-3, the γ values at the physiological salinity, e.g. 0.15 M NaCl are between 70 and 80% of those in absence of electrolyte. Therefore, the electrolytes in blood impeded the binding of RBR to HSA. From curves in Fig. (3B), γ at 37 °C approaches that at 20 °C. γ increases slightly when the temperature is more than 40 °C. On one hand, the peptide chain will expand when being heated, which could weaken its three-dimensional conformation [19] in such a way as to favor the insertion of organic molecules. On the other hand, such expansion will increase the distance between peptide chains. Thus, it will rearrange the effective binding points on the peptide chain and lead to the desorption of small organic substances [16, 20]. The balance between these mechanisms determines a final effect of temperature on the non-covalent interactions.

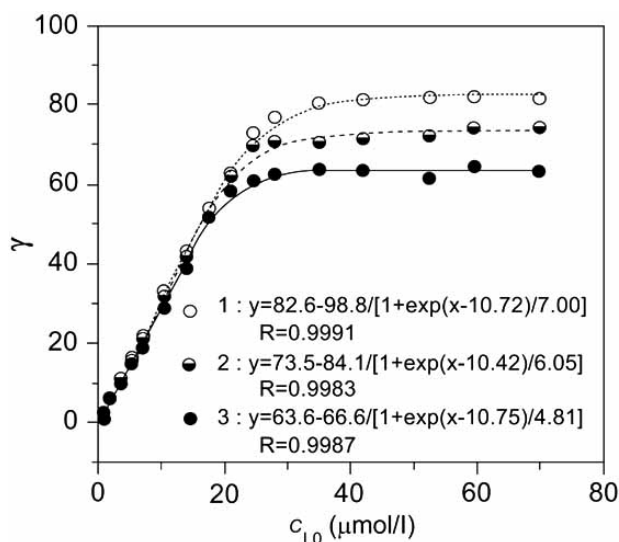


Figure 2. Variation of γ in solutions containing 0.02 mg/ml HSA and variable RBR (from 0.35 to 70 $\mu\text{mol/l}$). 1- pH 2.19, 2- pH 2.86 and 3- pH 3.39.

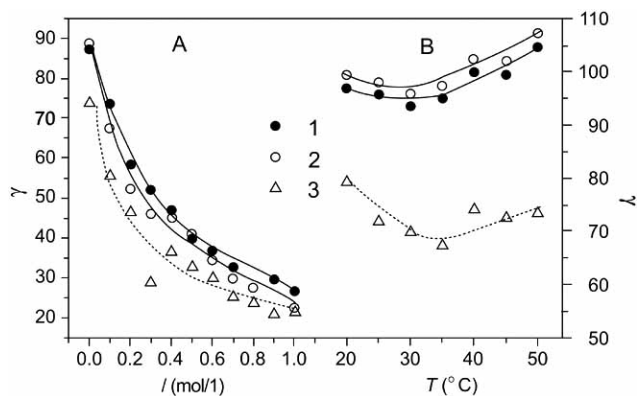


Figure 3. Effects of electrolyte (A) and temperature (B) on γ of solutions containing 0.042 mmol/l RBR and 0.02 mg/ml HSA at: 1- pH 2.19, 2- pH 2.86, and 3- pH 3.39.

Thermodynamic Characterization of the RBR-HSA Interaction

In order to understand the mechanism of the HSA-RBR reaction and to assess the effect of acidity, on its specificity and stability, a group of detailed thermodynamic data is indispensable. ITC measurements provide information on thermodynamic quantities such as enthalpy during the molecular interaction based on the heat produced by reactions [21, 22]. Fig. (4) depicts the typical isothermal titration curves obtained by injecting 2.5 mmol/l RBR into the ITC cell containing 2 $\mu\text{mol/l}$ HSA in three pHs media at 37 °C.

From curves X-1 (X=A, B, C), an exothermic heat pulse is detected following each injection. Its magnitude progressively decreases until a plateau is reached corresponding to the heat of dilution of the peptide species in the B-R buffer and indicating saturation. The heat involved at each injection was corrected for the heat of dilution, which was determined separately by injecting the RBR solution into the B-R buffer and then divided by the number of moles injected. The area of each peak was integrated and corrected as the enthalpy change (ΔH) of the reaction (curves X-2 in Fig. 4). The data appears to fit the cooperative model well in all three pH media, so the binding of RBR to HSA corresponds to a three-step sequential interaction. The first step occurs at c_{L0}/c_{M0} being less than 20, the second step at c_{L0}/c_{M0} between 20 and 40 and the third step at c_{L0}/c_{M0} being more than 40. The ΔH value in the first step was calculated by the relation:

$$\Delta H_1 = \frac{1}{N_1} \int_0^{20} \Delta H d(c_{L0}/c_{M0}), \text{ where } N_1 \text{ is the mole number of}$$

RBR binding to HSA in the first step at 20 of c_{L0}/c_{M0} , obtained from Fig. (2). The entropy change (ΔS) was calculated by the second law of thermodynamics $\Delta S = k(\Delta H/T)_R$ at the isothermal state, where k is the correction constant for the non-reversible reaction and T the temperature in Kelvin degrees. The stability constant (K_b) and the Gibbs free energy change (ΔG) in every step were then calculated using the equation $\Delta G = -RT \ln K_b = \Delta H - T\Delta S$, where R is the gas constant, $8.314 \text{ J}\cdot\text{mol}^{-1}\cdot\text{K}^{-1}$. According to the same way, the thermodynamic parameters, N , ΔG , K_b , ΔH and ΔS in the

second step were calculated, where $\Delta H_2 = \frac{1}{N_2} \int_{20}^{40} \Delta H d(c_{L0}/c_{M0})$.

All the results are given in Table 1.

Because all ΔH are much less than 60 kcal/mol [23], the RBR-HSA interaction is non-covalent, involving ionic interaction [24], hydrogen bond [25], hydrophobic interaction e.g. π - π stacking, dispersion force and van der Waals force, orientation force, where ion-pair interaction plays a position-fixing role. In the first step, all three ΔH_1 remain at the higher values between -1.68 and -3.03 kcal/mol. The binding of RBR may occur on the external surface of HSA via electric interaction e.g. $-\text{SO}_3^-$ of RBR with $-(\text{CH}_2)_4\text{NH}_3^+$ of K541 in subdomain IIIB and hydrogen bond e.g. $-\text{OH}$ of RBR with $-\text{COOH}$ of E542 (Fig. 5 - 1). All possible sites of RBR binding to HSA are listed in Table 2.

The union of non-covalent bonds caused a high ΔH . In the second step, the ΔH_2 is between -1.07 and -2.43 kcal/mol

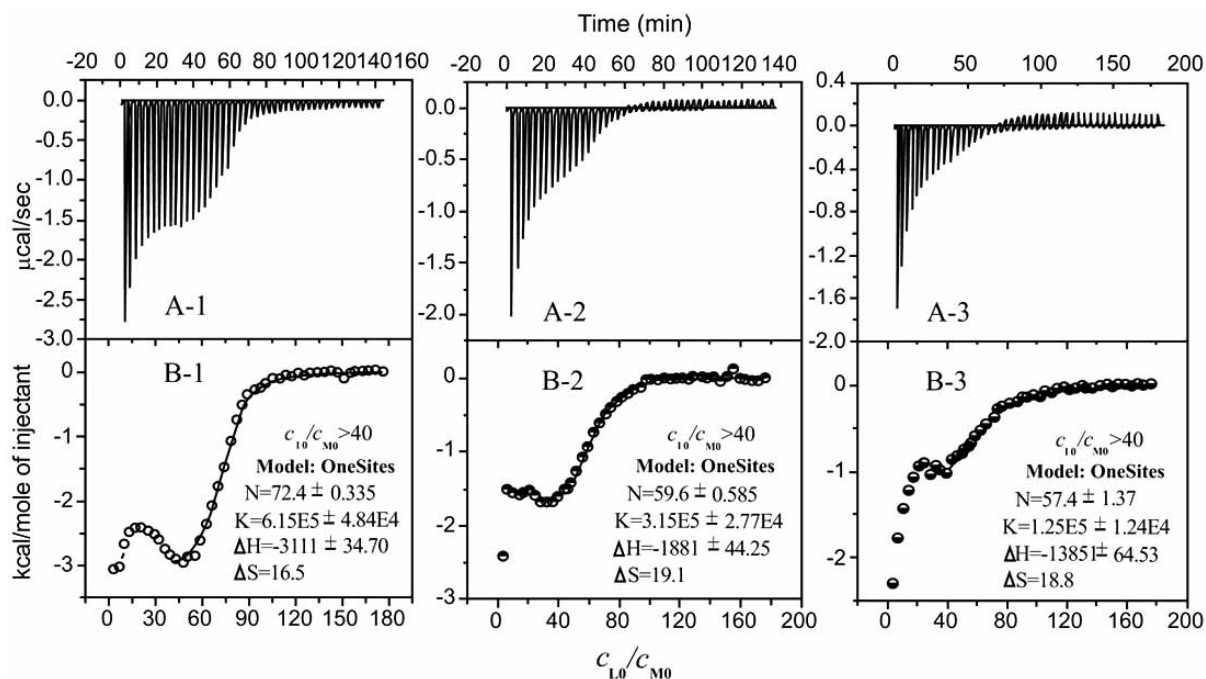


Figure 4. X-1 (X= A, B, C): ITC titration profile of RBR–HSA interaction at pH 2.19 (A), pH 2.86 (B) and 3.39 (C). The temperature was 37°C and all the solutions contained 10% B-R buffer. Each pulse corresponded to a 6- μ l injection of 2.5 mmol/l RBR into the ITC cell (1.4685 ml) containing 0.002 mmol/l HSA. X-2: The area of each peak in X-1 was integrated and corrected for the heat of dilution, which was estimated in a separate experiment by injecting the RBR into the B-R buffer. The corrected heat was divided by the moles of injectant and values were plotted as a function of c_{L0}/c_{M0} when $c_{L0}/c_{M0} > 40$.

Table 1. Determination of the Thermodynamic Parameters of the HSA-RBR Binding Reaction at pH 2.19, 2.86 and 3.39

pH	<i>i</i> -th	c_{L0}/c_{M0}	N_i	$K_{b,i} M^{-1}$	ΔH_b kcal/mol	ΔS_b cal/(mol K)	ΔG , kcal/mol
2.19	1	< 20	19	832	-3.03	3.6	-4.15
	2	20 - 40	18	15.2	-2.43	-2.43	-1.68
	3	> 40	35	6.15×10^5	-3.11	16.5	-8.23
2.86	1	< 20	18	6.85×10^3	-2.16	10.6	-5.45
	2	20 - 40	18	9.9	-1.69	-0.89	-1.41
	3	> 40	24	3.15×10^5	-1.88	19.1	-7.80
3.39	1	< 20	16	3.05×10^5	-1.68	19.7	-7.79
	2	20 - 40	18	4.2	-1.07	-0.61	-0.88
	3	> 40	23	1.25×10^5	-1.38	18.8	-7.21

but also the entropy decrease occurred with low values. The binding of RBR may still occur on the external surface of HSA via electric interaction e.g. $-\text{SO}_3^-$ of RBR with $-(\text{CH}_2)_4\text{NH}_3^+$ of K225 in subdomain IIA and hydrophobic interaction e.g. $-\text{Ar}$ of RBR with $-\text{CH}_2\text{Ar}$ of F223 (Fig. 5 - 2). By comparison of $K_{b,2}$ with $K_{b,1}$, the interaction of RBR in the second step is much weaker than that in the first step. It is attributed to the fact that the hydrophobic interaction is less than hydrogen bond. When c_{L0}/c_{M0} is more than 40, the interactions of RBR with HSA were fitted to a sigmoid curve by a nonlinear least squares method. The regression results are given in Table 1 as well. All N values corresponded to

those obtained from Fig. (2) if the electrolyte effect was corrected. The ΔH_3 is between -1.38 and -3.11 kcal/mol. The RBR anions may be attracted to insert the intracavity of HSA and then the polar groups ($-\text{SO}_3^-$, $-\text{OH}$, $-\text{N}=\text{N}-$ and $-\text{NH}-$) of RBR bound to the polar side chains located in the helix of HSA by hydrogen bond and the non-polar groups ($-\text{Ar}$ and $-\text{Ar N}_3\text{Cl}_2$) of RBR interacted with the hydrophobic groups exposed on the surface of HSA intracavity. For example, the $-\text{SO}_3^-$ of RBR fixed to $=\text{NH}_2^+$ of R197 in subdomain IIA via electric interaction, and then the $-\text{OH}$ of RBR bound to $-\text{NH}_2$ of Q196 by hydrogen bond [26], and the interaction via $-\text{Ar}$ of RBR with $-\text{ArOH}$ of Y452 in subdomain IIIA via π - π

Table 2. Possible Sites of RBR Binding to HSA at pH 2.19

Bind to the External Surface of HSA					Insert into the HSA Intracavity			
No	AAR for Position-Fixing	Polar AAR for Co-binding	AAR for Position-Fixing	Non-Polar or Aromatic AAR for co-Binding	No	AAR For Position-Fixing	No	AAR for Position-Fixing
1	R10	F11, K12, H9	K41	V40, L42, V43	1	H105, K106	19	H247
2	H39	D38, E37	K51	F53, F49	2	K136, K137	20	K286, H288
3	K64	D63, S65	H67	L66, L69	3	R144, R145	21	R336, R337
4	K73	D72	R114	L115	4	R146	22	H338
5	R81	E82, K83, L80	R117	V116	5	K159, R160	23	R348
6	R98	N99, E97	K128	H127	6	K162	24	K351
7	K174	D173	K225	F223	7	K181	25	K402
8	K233	S232	K262	Y263, L260	8	R186	26	R410
9	R257	D256	K276	L275	9	K190	27	K413, K414
10	K274	S273	R281	L283	10	K195	28	R428
11	K286	L284, E285	K317	Y319, V315	11	R197	29	K432
12	H288	S287	R323	F326	12	K199	30	K436
13	K313	D314, S312	K372	V373, Y370	13	K205	31	K439, H440
14	K359	E358, L357	K378	F377, L380	14	R209	32	K445, R446
15	H367	E368	K389	L387, Q390	15	K212	33	K519
16	K536	H535	K534	L532, V533	16	R218	34	K521
17	K541	E542	K545	L544, V548	17	R222	35	K524, K525
18	K557	E556, V555	K574	L575, V576	18	H242		
19	K564	E565, D563						

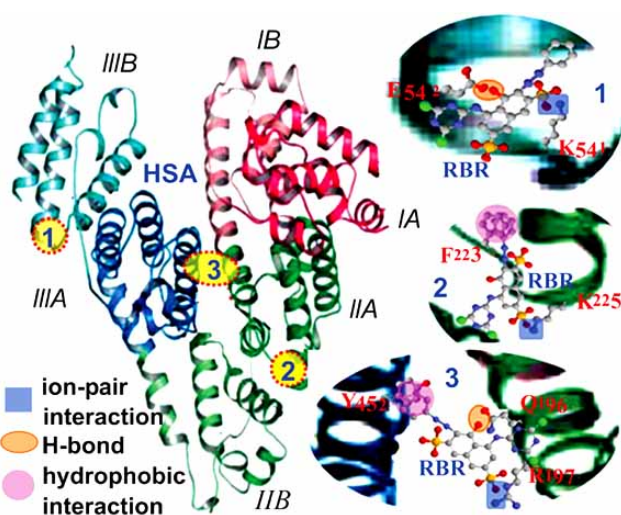


Figure 5. Cartoon illustrating the binding of RBR to amino acid residues through collective action of many non-covalent bonds e.g. electrostatic attraction, H- bonds and hydrophobic interaction.

stacking (Fig. 5 - 3). All possible binding sites of RBR are given in Table 2. By comparison of $K_{b,3}$ with both $K_{b,1}$ and $K_{b,2}$, the binding of RBR to the intracavity of HSA is the strongest. Moreover, the entropy increase is obvious in the three pH media, indicating that the unfolding of HSA conformation occurred in the high concentration solution of RBR. The possible reason is that RBR bridged between two subdomains of HSA e.g. IIA and IIIA (Fig. 5 - 3). From all of ΔG values, all the interactions of RBR with HSA are spontaneous. Without doubt, the binding of RBR will affect the physiological function of HSA e.g. transport transmission of the nutritional substances and drugs in blood.

Fluorescence Analysis of the RBR-HSA Interaction

Proteins contain Trp (W), Phe (F) and Tyr (Y) residues and its intrinsic fluorescence intensity depends on the degree of exposure of these residues to the polar, aqueous solvent and their proximity to specific quenching groups such as protonated carboxyl, protonated imidazole and deprotonated ϵ -amino groups [27]. The fluorescence of HSA at different pH values with the addition of RBR as quencher was obtained (Fig. 6). Results showed that a gradual decrease in the

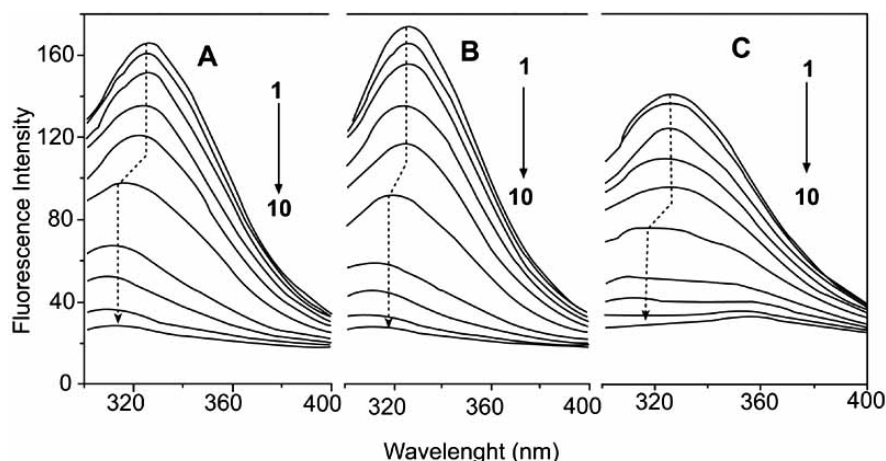


Figure 6. The fluorescence spectra of HSA-RBR solutions at pH 2.19 (A), pH 2.86 (B) and pH 3.39 (C) containing 0.1 mg/ml HSA. From 1 to 10: concentrations of RBR were 0.00, 0.35, 0.70, 1.40, 2.10, 3.50, 7.00, 10.5, 17.5 and 24.5 $\mu\text{mol/l}$.

fluorescence intensity of HSA was caused by quenching but there was no significant emission wavelength shift with the addition of c_{L0}/c_{M0} less than 35, which suggested that the microenvironment around tryptophan in HSA had not changed after interacting with RBR [13]. This also indicates the addition of RBR has not affect obviously the conformation of HSA when c_{L0}/c_{M0} is less than 35, i.e. RBR bound to the external surface of HSA, possible sites of RBR binding to HSA are F11, F223, Y263, Y319, F326, F377. However, the emission wavelength shift was obvious in the three pH media when c_{L0}/c_{M0} is more than 35. The high energy changes implied that RBR inserted the intracavity of HSA to result in the conformation change, and possible sites of RBR binding to HSA were F206, F211, W214, Y341, Y334, Y353, Y452, etc. This is consistent with the previous discussion on the ITC data.

Two models have been proposed for the quenching of protein fluorescence, static quenching and synthetic dynamic quenching. Dynamic (collisional) quenching results from the collisional encounters between the excited fluorophore and the quencher which may form a transitory encounter complex and then releases energy as heat [28]. The classical relationship often employed to describe the collisional (dynamic) quenching process by the Stern-Volmer equation [29]:

$$\frac{F_0}{F} = 1 + K_q \tau_0 c_L = 1 + K_{SV} c_L \quad (4)$$

where F_0 and F are the fluorescence intensities of HSA before and after the addition of the RBR, respectively, K_q the bimolecular rate constant for quenching, τ_0 the lifetime of the excited fluorophore in the absence of quencher. For biomacromolecules, τ_0 is approximately 10^{-8} s [29, 30], and K_{SV} is the Stern-Volmer quenching constant. Hence, Eq. 4 was applied to calculate K_q and K_{SV} by linear regression of plot F_0/F vs c_L . The data were shown in Table 3. Generally in dynamic quenching process, the highest collisional quenching constant of protein in the absence of most quenchers was about $2.0 \times 10^{10} \text{ l}\cdot\text{mol}^{-1}\cdot\text{s}^{-1}$ [31]. From Table 3, all K_q values are much higher than $2.0 \times 10^{10} \text{ l}\cdot\text{mol}^{-1}\cdot\text{s}^{-1}$. Thus, the interaction between RBR and HSA is a static quenching process.

Static quenching often obeys the Lineweaver-Burk equation [32, 33]:

$$\frac{1}{F_0 - F} = \frac{1}{F_0} + \frac{1}{K_A F_0 c_L} \quad (5)$$

where K_A is static quenching constant. From Table 3, all plots $(F_0 - F)^{-1}$ vs. c_L^{-1} are linear so the interaction between RBR and HSA is due to van der Waals force, electrostatic attraction, hydrophobic stack and their union [16].

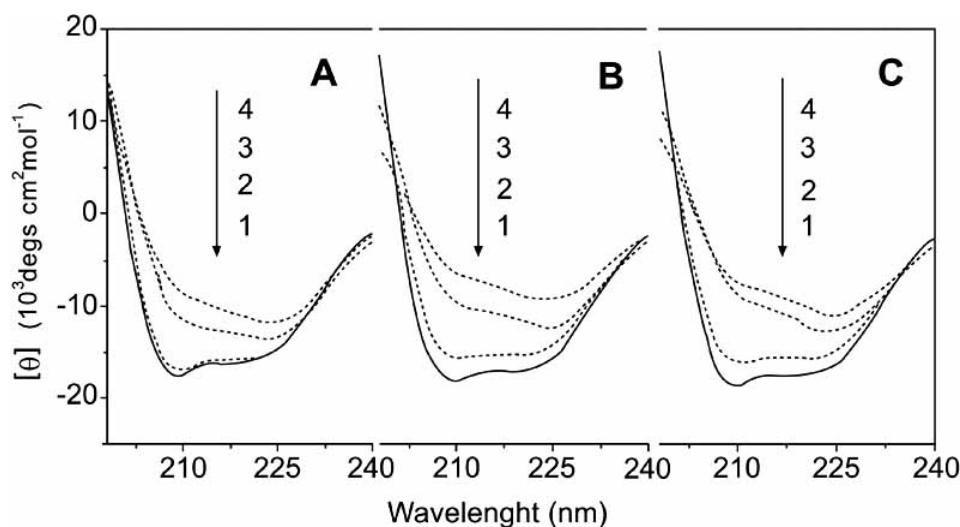
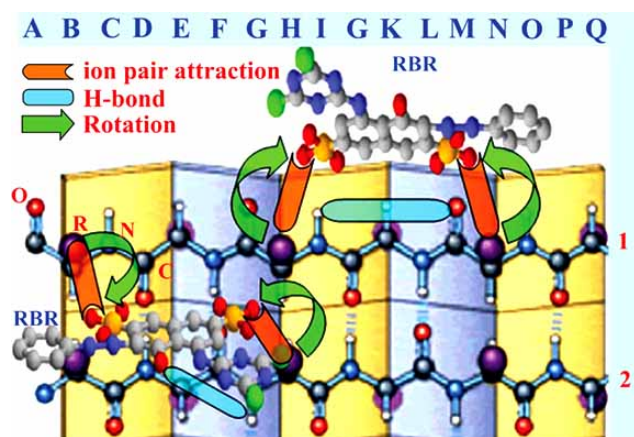
Change of HSA Conformation

The specific conformation of a protein with a particular function results from covalent and non-covalent interactions among its amino acid residues. When an organic compound such as a pollutant, drug or toxicant is added to a protein solution, the internal non-covalent interactions of the peptide chain may be altered or even destroyed. In particular, strong binding between a protein and an organic compound may cause a permanent and irreversible change in the conformation and the loss of its original function. CD spectrometry is often used to characterize the secondary structure of a protein [34, 35], i.e. the fractions of α -helix, β -sheet, β -turn and random coil. Variation of CD spectra of the solutions is shown in Fig. (7). The β -sheet of HSA always decreased with the increase of pH from 2.19 to 3.39 without RBR and α -helix increases. The increase of solution acidity caused the protonization of amino acid residues and destroyed the original internal hydrogen bonds to transfer the β -sheet of HSA into α -helix form.

The β -sheet fractions of HSA decreased rapidly in all three pH media with increasing concentrations of RBR. In contrast, the α -helix and β -turn fractions increased. For example, the β -sheet decreased by over 10% in 7 $\mu\text{mol/l}$ RBR at pH 2.86 and the β -turn increased from approximately 4 up to 10%. Similar results were obtained at pH 2.19 and 3.39. These phenomena confirmed that the binding of RBR to HSA transformed β -sheet into α -helix and β -turn forms with the addition of RBR. The decrease of β -pleated sheet fraction also indicated that the entropy decrease of the binding reaction and the folding of HSA [35]. Fig. (8) illustrates how

Table 3. Regression Equations and Fluorescence Quenching Constants of the Interaction between HSA and RBR

pH	Regression equation	K_{sv} ($l \cdot mol^{-1}$)	K_q ($l \cdot mol^{-1} \cdot s^{-1}$)
2.19	$F_0/F = 3.13 \times 10^5 c_{RBR} + 0.750$	3.13×10^5	3.13×10^{13}
	$(F_0 - F)^{-1} = 6.00 \times 10^{-8} c_{RBR}^{-1} - 0.002$		
2.86	$F_0/F = 2.53 \times 10^5 c_{RBR} + 1.09$	2.53×10^5	2.53×10^{13}
	$(F_0 - F)^{-1} = 6.00 \times 10^{-8} c_{RBR}^{-1} - 0.003$		
3.39	$F_0/F = 1.69 \times 10^5 c_{RBR} + 1.21$	1.69×10^5	1.69×10^{13}
	$(F_0 - F)^{-1} = 5.00 \times 10^{-8} c_{RBR}^{-1} + 0.005$		

**Figure 7.** The CD spectra of the HSA-RBR solutions at pH 2.19 (A), pH 2.86 (B) and pH 3.39 (C) containing 0.014 mg/ml HSA. From 1 to 4: RBR were 0.000, 0.007 and 0.014 mmol/l.**Figure 8.** Cartoon illustrating how the secondary structure of HSA may be changed in the presence of RBR.

the binding may effect changes from β -pleated sheet to helix and turn in the first process with little hydrophobic interaction. On a single peptide chain (chain 1), RBR could bridge the side groups (Rs) C_{N1} (rank N and line 1) and C_{H1} by ion-pair attraction. Thus, both the K-N and H-K sector sheets would rotate inversely around C_{K1} to split the original H-

bonds between chains 1 and 2, leading to the formation of an H-bond [26] between $C=O$ (M1) and NH (I1). In this way, the pleated sheet is transformed into β -turn. If both Rs were located on chains 1 and 2, such as C_{B1} and C_{H2} , the ion-pair attraction would draw both of them close to the two $-SO_3^-$ groups of RBR by inverse rotation. Because of the perturbation caused by RBR, the original H-bonds between chains 1 and 2 would be destroyed and a new H-bond between $-NH$ (G2) and $-OH$ of RBR formed. As a result, the β -sheet would be changed into a helix form [35, 36]. When concentration of RBR was over 0.014 mmol/l, the α -helix fraction decreased slowly (Fig. 7). The possible reason was the entry of RBR into the globular cavity in the third process caused the entropy increase of the binding reaction and the unfolding of HSA.

CONCLUSIONS

The objective of the study was to understand the general principle of the effect of non-specific binding of a sulfonic azo compound, RBR on HSA by using UV-VIS spectrometry, fluorophotometry, CD and ITC technique. The current work investigated the interactions of RBR with HSA and analyzed the potential toxic effect of RBR by determining RBR-HSA binding in the normal physiological acidities of skin and gastric tissues where RBR often presents. A three-

step binding model was found, in which the binding of RBR molecules might occur on the external surface of HSA via electric interaction when c_{L0}/c_{M0} is less than 40 and RBR molecules entered the hydrophobic intracavity of HSA when c_{L0}/c_{M0} is more than 40. Moreover, RBR binding result in a conformational change in structure of HSA even precipitation of HSA and inhibited its function accordingly. The possible binding site and the conformational transition of HSA were speculated and illustrated. This work provided a new insight into non-covalent interactions between azo compound and protein, which can be further used to investigate the potential toxicity mechanism of sulfonic azo dyes.

ACKNOWLEDGEMENTS

We sincerely thank the National Basic Research Program of China (973) (Grant No. 2010CB912604), State Key Laboratory Foundation of MSTC (PCRRY09004) & its Open Program (PCRRF08009) for financially supporting this work.

REFERENCES

- Binkowski, B.F.; Miller, R.A.; Belshaw, P.J. Ligand-regulated peptides: A general approach for modulating protein-peptide interactions with small molecules. *Chem. Biol.*, **2005**, *12*, 847-855.
- Creighton, T.E.; Kimb, P.S. Folding and binding. *Curr. Opin. Struct. Biol.*, **1991**, *1*, 3-4.
- Creighton, T.E. Stability of folded conformations. *Curr. Opin. Struct. Biol.*, **1991**, *1*, 5-16.
- Taboada, P.; Gutierrez-Pichel, M.; Mosquera, V. Effects of the molecular structure of two amphiphilic antidepressant drugs on the formation of complexes with human serum albumin. *Biomacromolecules*, **2004**, *5*, 1116-1123.
- Shaklai, N.; Garlick, R.L.; Bunn, H.F. Nonenzymatic glycosylation of human serum albumin alters its conformation and function. *J. Biol. Chem.*, **1984**, *259*, 3812-3817.
- Jia, Z.; Ramstad, T.; Zhong, M. Determination of protein-drug binding constants by pressure-assisted capillary electrophoresis (PACE)/frontal analysis (FA). *J. Pharm. Biomed. Anal.*, **2002**, *30*, 405-413.
- Matsushita, S.; Chuang, V.T.G.; Kanazawa, M.; Tanase, S.; Kawai, K.; Maruyama, T.; Suenaga, A.; Otagiri, M. Recombinant human serum albumin dimer has high blood circulation activity and low vascular permeability in comparison with native human serum albumin. *Pharmaceut. Res.*, **2006**, *23*, 882-891.
- Curry, S.; Mandelkew, H.; Brick, P.; Franks, N. Crystal structure of human serum albumin complexed with fatty acid reveals an asymmetric distribution of binding sites. *Nat. Struct. Biol.*, **1998**, *5*, 827-835.
- Bianchini, R.; Pinzino, C.; Zandomenighi, M. Interaction of a reactive dye with serum albumins and with aminoacids: the dye as a chiral label. *Dyes Pigments*, **2002**, *55*, 59-68.
- Silva, D.; Cortez, C.M.; Cunha-Bastos, J.; Louro, S.R.W. Methyl parathion interaction with human and bovine serum albumin. *Toxicol. Lett.*, **2004**, *147*, 53-61.
- Uddin, S.J.; Shilpi, J.A.; Murshid, G.M.M.; Rahman, A.A.; Sarder, M.M.; Alam, M.A. Determination of the binding sites of arsenic on bovine serum albumin using warfarin (site-I specific probe) and diazepam (site-II specific probe). *J. Biol. Sci.*, **2004**, *4*, 609-612.
- Skipper, P.L.; Tannenbaum, S.R. Molecular dosimetry of aromatic-amines in human-populations. *Environ. Health Persp.*, **1994**, *102*, 17-21.
- Zhang, X.; Chen, L.; Fei, X.C.; Ma, Y.S.; Gao, H.W. Bindings of PFOS to serum albumin and DNA: Insights into the molecular toxicity of perfluorochemicals. *BMC Mol. Biol.*, **2009**, *10*, 16.
- Gao, H.W.; Zhao, J.F.; Yang, Q.Z.; Liu, X.H.; Chen, L.; Pan, L.T. Non-covalent interaction of 2', 4', 5', 7'-tetrabromo-4, 5, 6, 7-tetrachlorofluorescein with proteins and its application. *Proteomics*, **2006**, *6*, 5140-5151.
- Ghuman, J.; Zunszain, P.A.; Petitpas, I.; Bhattacharya, A.A.; Otagiri, M.; Curry, S. Structural basis of the drug-binding specificity of human serum albumin. *J. Mol. Biol.*, **2005**, *353*, 38-52.
- Gao, H.W.; Zheng, L.X.; Mei, H.D. Aggregation of a dye on a surfactant: Interaction of coomassie brilliant blue G250 with cetyltrimethylammonium bromide and determination of the cationic surfactant in water. *Instrument. Sci. Technol.*, **2004**, *32*, 271-280.
- Malkov, V.A.; Voloshin, O.N.; Soyfer, V.N.; Frankkamenetskii, M.D. Cation and sequence effects on stability of intermolecular pyrimidine-purine-urine triplex. *Nucleic Acids Res.*, **1993**, *21*, 585-591.
- Quinn, S.J.; Kifor, O.; Trivedi, S.; Diaz, R.; Vassilev, P.; Brown, E. Sodium and ionic strength sensing by the calcium receptor. *J. Biol. Chem.*, **1998**, *273*, 19579-19586.
- Boscolo, B.; Leal, S.S.; Ghibaudi, E.M.; Gomes, C.M. Lactoperoxidase folding and catalysis relies on the stabilization of the alpha-helix rich core domain: A thermal unfolding study. *BBA-Protein. Proteom.*, **2007**, *1774*, 1164-1172.
- Gao, H.W.; Liu, X.H.; Qiu, Z.; Tan, L. Non-covalent binding of azo compound to peptide chain: interactions of biebrich scarlet and naphthochrome green with four model proteins. *Amino Acids*, **2009**, *36*, 251-260.
- Goobes, R.; Minsky, A. Contextual equilibrium effects in DNA molecules. *J. Biol. Chem.*, **2001**, *276*, 16155-16160.
- Cooper, A.; Mcalpine, A.; Stockley, P.G. Calorimetric studies of the energetics of protein-DNA interactions in the *E. coli* methionine repressor (MetJ) system. *FEBS Lett.*, **1994**, *348*, 41-45.
- Gao, H.W.; Xu, Q.; Chen, L.; Wang, S.; Wang, Y.; Wu, L.L.; Yuan, Y. Potential protein toxicity of synthetic pigments: Binding of poncean S to human serum albumin. *Biophys. J.*, **2008**, *94*, 906-917.
- Gao, H.W.; Qian, Y.; Hu, Z.J. Tetraiodophenolsulfonphthalein as a spectral substitute to characterize the complexation between cationic and anionic surfactant. *J. Colloid Interf. Sci.*, **2004**, *279*, 244-252.
- Panigrahi, S.K.; Desiraju, G.R. Strong and weak hydrogen bonds in the protein-ligand interface. *Proteins-Struct. Funct. Bioinf.*, **2007**, *67*, 128-141.
- Kortemme, T.; Morozov, A.V.; Baker, D. An orientation-dependent hydrogen bonding potential improves prediction of specificity and structure for proteins and protein-protein complexes. *J. Mol. Biol.*, **2003**, *326*, 1239-1259.
- Marty, A.; Boiret, M.; Deumie, M. How to illustrate ligand-protein binding in a class experiment - an elementary fluorescent assay. *J. Chem. Educ.*, **1986**, *63*, 365-366.
- Behera, G.B.; Mishra, B.K.; Behera, P.K.; Panda, M. Fluorescent probes for structural and distance effect studies in micelles, reversed micelles and microemulsions. *Adv. Colloid Interfac.*, **1999**, *82*, 1-42.
- Gratton, E.; Jameson, D.M.; Weber, G.; Alpert, B. A model of dynamic quenching of fluorescence in globular-proteins. *Biophys. J.*, **1984**, *45*, 789-794.
- Weber, G. The Quenching of Fluorescence in Liquids by Complex Formation - Determination of the Mean Life of the Complex. *Trans. Faraday Soc.*, **1948**, *44*, 185-189.
- Ware, W.R. Oxygen quenching of fluorescence in solution - an experimental study of diffusion process. *J. Phys. Chem.*, **1962**, *66*, 455-458.
- Lakowicz, J.R.; Weber, G. Quenching of protein fluorescence by oxygen - detection of structural fluctuations in proteins on nanosecond time scale. *Biochemistry*, **1973**, *12*, 4171-4179.
- Lehrer, S.S. Solute perturbation of protein fluorescence - quenching of tryptophyl fluorescence of model compounds and of lysozyme by iodide ion. *Biochemistry*, **1971**, *10*, 3254-3263.
- Dockal, M.; Carter, D.C.; Ruker, F. Conformational transitions of the three recombinant domains of human serum albumin depending on pH. *J. Biol. Chem.*, **2000**, *275*, 3042-3050.
- Era, S.; Sogami, M. H-1-NMR and CD studies on the structural transition of serum albumin in the acidic region - The N -> F transition. *J. Pept. Res.*, **1998**, *52*, 431-442.
- Carter, D.C.; Ho, J.X. Structure of serum-albumin. *Adv. Protein Chem.*, **1994**, *45*, 153-203.